5-2011

A Singular Perturbation Approach to the Fitzhugh-Nagumo PDE for Modeling Cardiac Action Potentials.

Jeremy Brooks
East Tennessee State University

A Singular Perturbation Approach to the Fitzhugh-Nagumo PDE for Modeling Cardiac Action Potentials

Thesis submitted in partial fulfillment of Honors

By

Jeremy Brooks
The Honors College
University Honors Scholars Program
Honors-in-Discipline, Department of Mathematics and Statistics
East Tennessee State University

29 April 2011

Dr. Jeff Knisley, Faculty Mentor

A Singular Perturbation Approach to the Fitzhugh-Nagumo PDE for Modeling Cardiac Action Potentials

Jeremy Brooks

29 April 2011

Abstract

The study of cardiac action potentials has many medical applications. Dr. Dennis Noble first used mathematical models to study cardiac action potentials in the 1960s. We begin our study of cardiac action potentials with one form of the Fitzhugh-Nagumo partial differential equation. We use the non-classical method to produce a closed form solution for the decoupled Fitzhugh Nagumo equation. Using voltage recording data of action potentials in a cardiac myocyte and in purkinje fibers, we estimate parameter values for the closed form solution with standard linear and non-linear regression methods. Results are limited, thus leading us to perturb the solution to obtain a better fit. We turn to singular perturbation theory to justify our pole-based approach. Finally, we test our model on independent action potential data sets to evaluate our model and to draw conclusions on how our model can be applied.

1 Acknowledgment

I would like to thank my thesis advisor, Dr. Jeff Knisley, for his great assistance in this project. Although Dr. Knisley's research focus is in neuron action potentials, he put much time and effort into learning the subtleties of modeling cardiac action potentials with me. Dr. Knisley patiently and unfailingly provided me guidance during the project and helped me with problems that arose while writing the computer code for the model. I am

also grateful for his lectures on singular perturbation theory, without which I would have been unable to successfully model a myocyte action potential. Finally, I thank him for our many conversations on the differences between cardiac and neuron action potentials and our discussions on life, in general.

2 Introduction

Cardiac arrhythmias occur commonly in the general population. Arrhythmias are defined as any change in the normal sequence of the heart's electrical impulses that lead to abnormal heart rhythms [2]. While some people are affected by a short, non-threatening period of an arrhythmia, other people suffer from prolonged arrhythmias that lead to discomfort and in some cases death. For example, the American Heart Association reports that 2.2 million Americans suffer from atrial fibrillation. Atrial fibrillation occurs when the heart's electrical conduction system falters, and instead of being regulated by the sinoatrial node, both atria are subject to erratic electrical impulses. This causes the atria to essentially quiver, preventing the ventricles from filling completely. Atrial fibrillation and other arrhythmias can lead to more serious and life-threatening heart conditions [3]. Additionally, arrhythmias can lead to sudden cardiac death [4]. Consequently, much effort and resources have been put into researching cardiac arrhythmias.

One tool for better understanding these arrhythmias is mathematical models of cardiac action potentials which may be used to study the interplay of the different ions responsible for conducting electrical impulses throughout the heart. In addition to leading to advances in the etiology and treatment of cardiac arrhythmias, mathematical models have the potential to aid in the testing of new pharmaceutical drugs that target proteins involved in cardiac repolarization. These drugs can have fatal arrhythmic side-effects [5].

We begin by examining the physiology of cardiac action potentials. We then briefly look at the history of mathematical cardiac action potential models before building our own mathematical model.

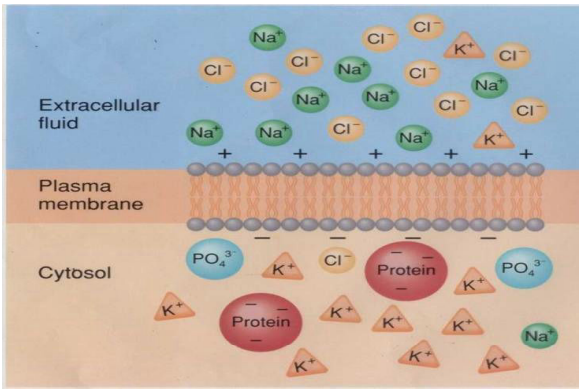

Figure 1: Potential across cell membrane. The difference in ion concentration, or electrical charge, enables the cell to communicate with the rest of the body via action potentials [6].

3 Cardiac Action Potential

Cardiac cells, similar to neurons and muscular cells, are excitable cells. That is, they can generate and respond to electrical impulses. This is possible because of the membrane potential across their cell membranes. The cell membrane is composed of a semipermeable phospholipid bilayer, enabling the cell to control which substances, such as ions, can pass into and out of the cell. At any given time, there is a different concentration of ions and, consequently, an electrical charge inside and outside of the cell (see Figure 1). Thus, the cell has a membrane potential and the cell membrane can be thought of as an electrical capacitor that can hold a charge. This electrical charge can be discharged by movement of ions across the cell membrane. This movement of ions and change in membrane potential is called an action potential. Action potentials enable cells to communicate with each other and send information throughout the body [7, 1].

The membrane potential is calculated relative to the charge inside the cell as $V_{in} - V_{out}$, where V_{in} is the charge due to ions inside the cell and V_{out} is the charge due to ions outside the cell. Table 1 shows the most common ions associated with cardiac cells and their concentrations inside and outside the cell. Note that sodium (Na^+), potassium (K^+), and calcium (Ca^{2+}) are responsible for the action potential as will be described below. Also note the

Table 1			
Ion	Extracellular (mM)	Intracellular (mM)	Nernst Potential (mV)
Na^+	145	15	60
Cl^-	100	5	-80
K^+	4.5	160	-95
Ca^{2+}	1.8	0.0001	130
H^+	0.0001	0.0002	-18

Table 1: Ion concentrations in most cardiac cells [1].

particular importance of calcium, which stimulates the actual contraction of the cardiac cell during a heartbeat [8].

It is also important to note the difference between pacemaker cardiac cells and non-pacemaker cardiac cells. Pacemaker cells make up the sinoatrial node and pace the heart. They have a slower rate of depolarization and their action potential is carried out via a slightly different pathway [10]. We will focus on non-pacemaker cardiac cells in our model. From here on, when we say cardiac cell, we are referring to non-pacemaker cells.

There are two main types of non-pacemaker cardiac cells, see Figure 3: Purkinje fiber cells and myocardial cells. Purkinje fiber cells are used to quickly conduct electrical signals throughout the heart in order to activate the myocardium to contract. Myocardial cells are the muscle cells of the heart that actually contract during heart beats. Both cell types have similar action potentials that last approximately 500 msec [1].

The resting potential of cardiac cells is approximately -90 mV, as seen in Figure 2. That is, there is more positive charge outside the cell than inside, as depicted in Figure 1. Like all other excitable cells, a cardiac cell will not have an action potential until the membrane potential reaches a threshold value. This prevents small, random electrical impulses from triggering an excitable cell. For cardiac cells, the threshold voltage potential is -70 mV. A cell is depolarized to its threshold when a neighboring cell has an action potential and sends an electrical impulse to the cell. Once a cell hits the threshold, Na^+ channels in the cell's phospholipid bilayer open up allowing Na^+ ions to rush into the cell along the electrical gradient, as seen in Phase

0 in Figure 2. At the same time, the K^+ channels are closed, preventing K^+ ions from leaving the cell. The cardiac cell continues to depolarize until the membrane potential is approximately +25 mV. At this point, the Na^+ channels close, and the K^+ channels open back up, allowing some of the positively charged potassium ions to leave the cell and reduce the membrane potential, as illustrated by Phase 1 in Figure 2. This is the start of repolarization. However at the same time K^+ leaves the cell, slow inward Ca^{2+} channels open, allowing positive Ca^{2+} ions to flow into the cell. This leads to the signature plateau phase of cardiac action potentials: the in-flowing Ca^{2+} cells slow down the repolarization effect of the out-flowing K^+ ions for approximately 200 ms, which is denoted as Phase 2 in Figure 2 [8]. Repolarization is completed as the Ca^{2+} channels are inactivated and the outflowing K^+ ions lower the membrane potential to its resting value, which is Phase 3 in Figure 2. The cardiac cell is then ready to wait for the next electrical impulse from neighboring cells. Finally, we note that cardiac cells have an effective refractory period, consisting of phases 0,1,2 and part of 3, in which the cell cannot be stimulated by a neighboring cell to produce another action potential. The effective refractory period serves as a safety check, ensuring that the chambers of the heart have enough time to fill with and then pump blood [9].

4 Cardiac AP vs Neuron AP

In general, when one hears the term action potential he or she associates the term with a neuron. Here we point out the difference in action potentials in the two cell types. Figure 4 clearly shows how much shorter a neuron AP is compared to a myocyte AP. This is due to the unique plateau phase in myocytes caused by the slow Ca^{2+} ion channels. Functionally, it is sensible that a myocyte AP would be longer than a neuron AP. Consider, for example, two individuals, A and B, standing at opposite ends of a football field with other people standing in between them. If person A sees that the scoreboard is about to fall on person B, both of them want individual A to pass that information to individual B as quickly as possible. Conversely, if person A is selling cups of lemonade on a hot, fall afternoon, then person B wants to get his lemonade in a timely manner but person B is fine with people slowly passing his lemonade to him so that it does not spill. Similarly, neurons are responsible for quickly sending information between the brain and body and

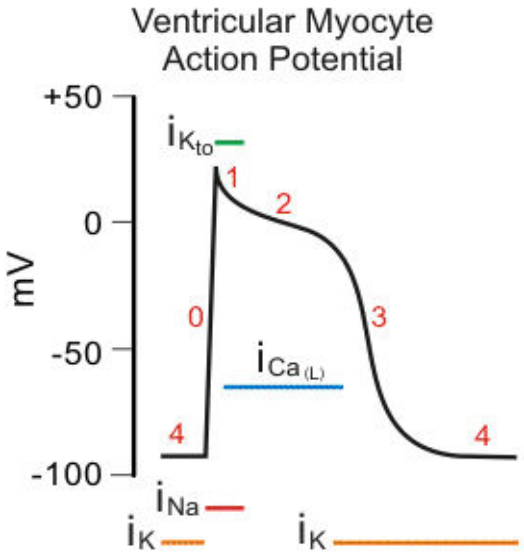

Figure 2: Action potential in a ventricular myocyte. The plot denotes when specific ion channels are open during an action potential [9].

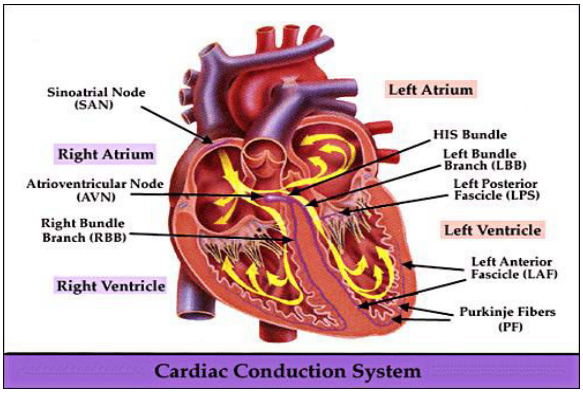

Figure 3: During each heart beat, electrical impulses originate in the SA node and then travel through the heart as seen in the image. Purkinje fibers are responsible for quickly conducting electrical impulses around both ventricles, stimulating the ventricles to contract at the same time. Myocardial cells make up the heart wall and contract in order for the heart to pump blood throughout the body [11].

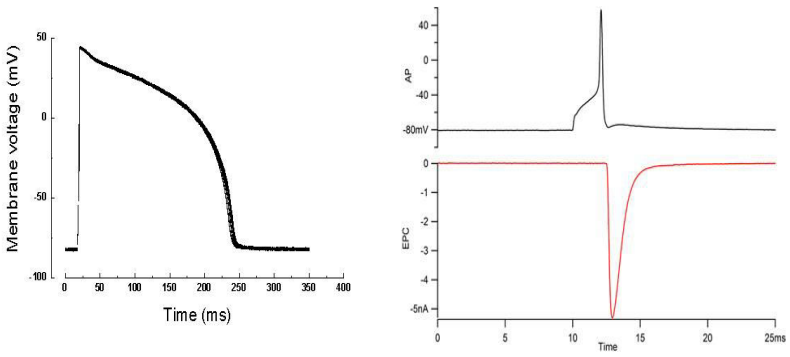

Figure 4: On the left is an action potential from a single guinea pig ventricular myocyte [12]. On the top right is an action potential from a motor neuron [19]. The myocyte AP is approximately 225 msec compared to the neuron AP which lasts less than 5 msec. Also note the lack of a plateau phase in the neuron AP.

speed is of the essence. While myocytes also need to propagate electrical signals with speed, their action potentials must also last long enough for cellular contraction and for the atria and ventricles to have enough time to completely fill with blood in diastole and empty during systole.

As discussed earlier, the heart is composed of several cell types - nodal cells, Purkinje Fibers, myocardial cells, and more. Each of these have a slightly different function and, consequently, slightly different action potentials. This diversity coupled with the many different ionic channels found in cardiac cells make it challenging to model cardiac action potentials. Thus, like most mathematical models, there is a fine line that one must evaluate between modeling every detail of the process and leaving out inconsequential components of a myocyte action potential [1].

5 Mathematical Models of Action Potentials

5.1 Hodgkin-Huxley

The first mathematical model of action potentials was completed by Alan Lloyd Hodgkin, Andrew Fielding Huxley, and Bernard Katz. They measured the ionic current in a giant axon of a squid using a voltage clamp and new

techniques they developed. They made two key assumptions. First, Hodgkin and Huxley assumed "that the initial inward current is carried almost entirely by Na+ ions, while the outward current that develops later is carried largely by K+ ions" [1]. Second, they inferred that "the potassium channels are unaffected by the change in extracellular sodium concentration" [1]. Their data suggested that the action potential consisted of four processes: change in membrane potential $v(t)$, potassium activation $n(t)$, sodium activation $m(t)$, and sodium inactivation $h(t)$, where t is the time [1]. Analyzing these four processes, Hodgkin and Huxley developed four ordinary differential equations (ODEs) to mathematically describe the action potential [1]:

$$C_m \frac{dv}{dt} = -g_k(v - v_k)n^4 - g_{Na}(v - v_{Na})m^3h - g_L(v - v_L) + I_{app} \quad (1)$$

$$\frac{dm}{dt} = \alpha_m(1 - m) - \beta_m m \quad (2)$$

$$\frac{dn}{dt} = \alpha_n(1 - n) - \beta_n n \quad (3)$$

$$\frac{dh}{dt} = \alpha_h(1 - h) - \beta_h h \quad (4)$$

where v is the change in membrane potential, m is the Na^+ channel activation rate, n is the K^+ channel activation rate, h is the Na^+ channel inactivation rate, and g is the conductance of the denoted ion channel.

5.2 Cardiac Models

After Hodgkin and Huxley's work was published, mathematicians and scientists began working to model other excitable cells, including cardiac cells. In 1962, Denis Noble published the first mathematical model of cardiac action potentials. His model was an extension of the Hodgkin-Huxley system of differential equations. His extension was based on a discovery that he and Otto Hunter made concerning potassium channels in purkinje fibers. This highlights the great extent of intellectual exchange between biochemistry and mathematics. Throughout the last 50 years of modeling myocyte action potential, and even longer for excitable cells in general, biologists have shared their experimental discoveries with mathematicians, who improved their models and offered insights into what areas the biologists should explore next. This integration of the sciences has led to remarkable leaps in the field of cardiac electrophysiology [5, 20].

Numerous experimental results, including Reuter's discovery of the Ca^{2+} in the late 1960s greatly improved mathematical models of cardiac action potentials. These developments led to the McAllister-Noble-Tsien Purkinje fiber model in 1975, the Beeler and Reuter model of a ventricular myocyte in 1977, and eventually, after other experimental discoveries, the Luo-Rudy models of guinea pig ventricular myocytes in the early 1990s. Later the discovery of a Na^+ and Ca^{2+} exchanger led to the DiFrancesco-Noble model of Purkinje fiber cells in 1985 and the Hilgemann-Noble model of atrial cells in rabbits in 1987. These two models became the basis for modern models of excitation-contraction coupling. In addition to guinea pig and rabbit models, mathematical models of cardiac action potentials have been developed for humans, canines, and rats, since the late 1990s [5, 21].

As a final note, we point out that many of these mathematical models were expressed as ODEs. We choose to express our model as a partial differential equation (PDE).

5.3 Fitzhugh-Nagumo

The Hodgkin-Huxley system of ODEs provide a physiologically accurate portrait of the action potential since they are obtained from actual measurements. However, they are not trivial to work with when modeling because they are highly nonlinear with sensitive dependence on the individual values of their many parameters. For this reason, scientists looked for a simpler model that retains the qualitative features of the Hodgkin-Huxley equations. In the 1960s, Richard Fitzhugh, a biophysicist, developed such a mathematical model based on the fast-slow phase-plane of the Hodgkin-Huxley system. Concurrently, Nagumo built an electrical circuit that modeled the phenomenon that Fitzhugh described mathematically. His electrical circuit consisted of a capacitor, a tunnel diode as a non-linear current-voltage device, and a resistor, inductor, and battery in series [1].

Fitzhugh and Nagumo were able to describe an action potential with two equations and two variables – a fast, excitation variable ν and a slow, recovery variable ω. Their model can be derived in several different ways, but we chose to start with the following two PDEs [1]. We next derive the single Fitzhugh-Nagumo PDE that we will use to build our model of a cardiac action potential.

$$\epsilon \frac{\partial \nu}{\partial t} = \epsilon^2 \frac{\partial^2 \nu}{\partial x^2} + \nu(1-\nu)(a-\nu) - \omega \tag{5}$$

$$\frac{\partial \omega}{\partial t} = \nu - \gamma\omega - \nu_0 \tag{6}$$

where ν_0 is the resting membrane potential and ϵ, γ, and a are positive constants. Note t is time and x is the distance along the myocyte membrane from a given starting point. We assume $\nu_0 = 0$. We will see later that this is justified because we can use a linear transformation to make the membrane voltage be between 0 and 1.

Notice in Equations 5 and 6 that ϵ is independent of time t and position x. Hence, we can rewrite the equations placing ϵ in the differential:

$$\frac{\partial \nu}{\partial (t/\epsilon)} = \frac{\partial^2 \nu}{\partial (x/\epsilon)^2} + \nu(1-\nu)(a-\nu) - \omega \tag{7}$$

$$\frac{\partial \omega}{\partial t} = \nu - \gamma\omega \tag{8}$$

Next, let $T = t/\epsilon$ and $X = x/\epsilon$.

$$\frac{\partial \nu}{\partial T} = \frac{\partial^2 \nu}{\partial X^2} + \nu(1-\nu)(a-\nu) - \omega \tag{9}$$

$$\frac{\partial \omega}{\partial T} = \epsilon(\nu - \gamma\omega) \tag{10}$$

Because ϵ is not on the left side of Equation 8, we multiply the right side of Equation 10 by ϵ.

As $\epsilon \to 0$ in Equation 10, $\frac{\partial \omega}{\partial T} \to 0$. Thus, w is a constant, and we let $w = 0$, arriving at the single Fitzhugh-Nagumo PDE, Equation 11. Physiologically, this assumption is valid since the recovery variable is non-existent at the beginning of an action potential.

$$\frac{\partial u}{\partial t} = \frac{\partial^2 u}{\partial x^2} + u(1-u)(a-u) \tag{11}$$

When we derive our model of a cardiac action potential below, we will begin with this PDE. The single Fitzhugh-Nagumo PDE describes the fast currents of the action potential, but we will have to modify the equation in order to model the entire action potential.

6 Methods

There is much interest in mathematical models of cardiac action potentials because of the insight they give into the interaction between fast and slow ion currents that generate the action potential. The robust nature of cardiac myocytes, evidenced in Figure 5, makes them good candidates for study by deterministic mathematical models. Since the interaction between the fast currents and slow currents occur in the same region in each AP, we can use models to study how the currents work, that is, when does each current turn on and off and which current overrides another. The goal of this study is to generate a mathematical model for cardiac AP's and then use the model to determine what causes the plateau phase that is unique to cardiac AP's and what ends the plateau phase, bringing the myocyte back to its resting potential.

Cardiac action potentials have been mathematically modeled for forty years; however, little work has been attempted in modeling cardiac AP's with partial differential equations. We build our mathematical model based on the Fitzhugh-Nagumo partial differential equation:

$$\frac{\partial u}{\partial t} = \frac{\partial^2 u}{\partial x^2} + u(1-u)(a-u) \tag{12}$$

It has been shown that a solution to the fast part of the Fitzhugh-Nagumo PDE, corresponding to the sharp depolarization in action potentials (See phase 0 in Figure 2), is given by [18]:

$$U(x,t) = \frac{Ae^{z_1} + aBe^{z_2}}{Ae^{z_1} + Be^{z_2} + C} \tag{13}$$

where U is the voltage at position x and time t, $z_1 = \frac{x}{\sqrt{2}} + (\frac{1}{2} - a)t$, $z_2 = \frac{ax}{\sqrt{2}} + a(\frac{a}{2} - 1)t$, and A, B, and C are arbitrary constants.

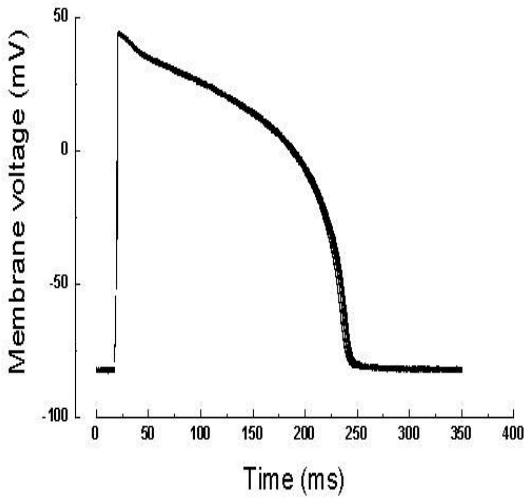

Figure 5: Superposition of 10 consecutive action potentials in a single guinea pig ventricular myocyte measured under standard conditions [12].

We verified that Equation 13 is indeed a solution to the Fitzhugh-Nagumo PDE in the mathematics software program *Maple 14*. In order to model the slow ion currents responsible for the repolarization of myocytes, we use a singular perturbation approach, outlined below and given in detail in the Appendix, to justify a more general form of Equation 13, which we derive below.

6.1 Data

We used three different sets of cardiac myocyte data in building our mathematical model. The first data set, shown in Figure 6, was obtained from a left ventricular myocyte of a pig. The second AP data was simulated from Noble's Purkinje Model and is shown in Figure 7. The third AP data was from a single guinea pig ventricular myocyte and was shown in Figure 5. These three data sets were chosen based on their robustness, the credibility of their source, and their span of different types of non-pacemaker cardiac cells.

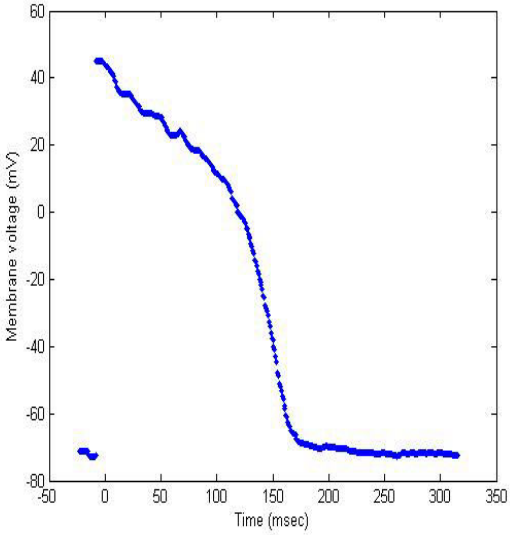

Figure 6: Action potential from a pig ventricular myocyte [13].

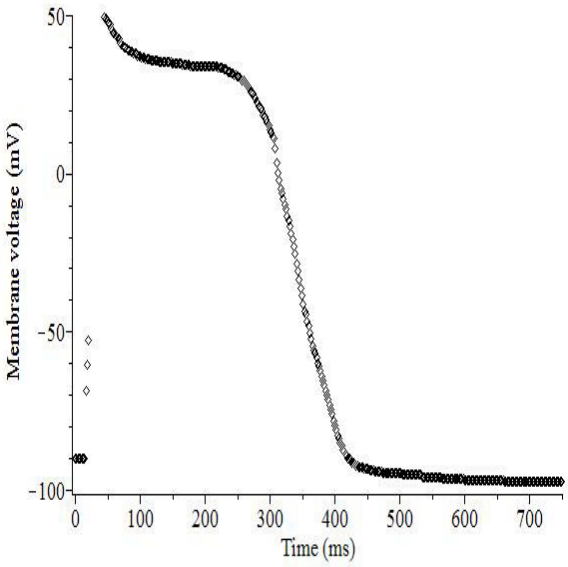

Figure 7: Simulated action potential from Noble's model of action potentials in purkinje fibers [14].

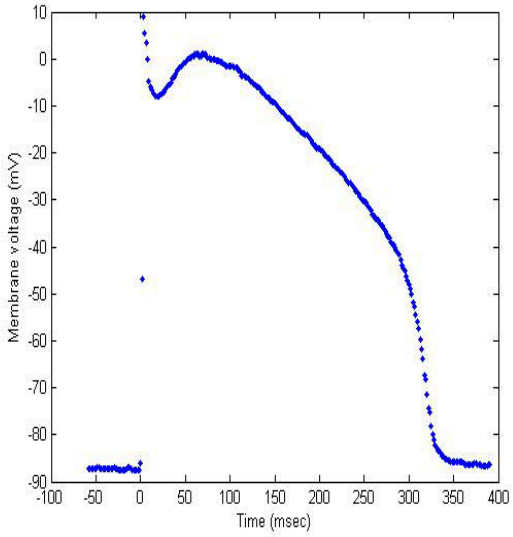

Figure 8: Action potential from a canine myocyte [15].

After building our mathematical model, we tested the model on a canine action potential, shown in Figure 8. We chose to independently test our model on the canine data set because of the sharp turn between the plateau phase and the repolarization phase, which signifies a distinct change in the dynamics of the ion currents. We hope to learn something about the interaction between the Ca^{2+} and K^{+} currents at this point in the action potential.

Finally, we ran our model with data from a failing canine myocyte to see if any of our parameters might preventively indicate a problem in a myocyte. The failing canine data set is shown in Figure 9.

Note, we converted the data sets into units of millivolts and milliseconds if they were not already in these units. Additionally, all of our analysis was completed in these units. We also rescaled the data sets such that membrane voltage was between 0 and 1. Since this is a linear transformation, the information we derive from the rescaled data in our model can be applied to the original data via the inverse of our linear transformation.

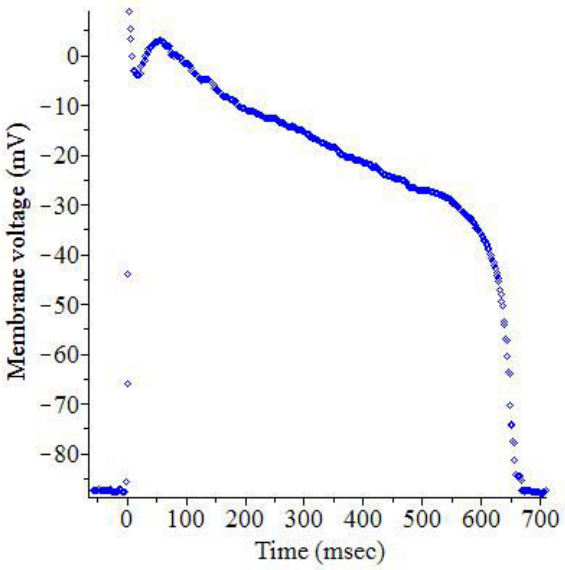

Figure 9: Action potential from a failing canine myocyte [15].

As a final note, when running our model on the data sets, we only worked with the data from the peak of the depolarization through the return to resting potential. This is illustrated in Figure 10. We ignored the depolarization phase for two reasons. First, the depolarization phase consists of a small number of points, usually less than five. Second, the depolarization phase occurs rapidly and is thus hard to model.

6.2 Deriving Our Model

An immediate goal is to obtain a fit for our data. If we multiply U by $\frac{\frac{1}{A}e^{-z_1}}{\frac{1}{A}e^{-z_1}} = 1$, we obtain:

$$U(x,t) = \frac{1 + aB_1e^{z_2-z_1}}{1 + B_1e^{z_2-z_1} + C_1e^{-z_1}} \tag{14}$$

where $B_1 = \frac{B}{A}$ and $C_1 = \frac{C}{A}$.

But $z_2 - z_1 = \frac{x}{\sqrt{2}}(a-1) + (\frac{a^2}{2} - \frac{1}{2})t$. If we assume that the voltage is constant over the length of the cardiac myocyte, then voltage is independent of x and U becomes a single variable function, only depending on t:

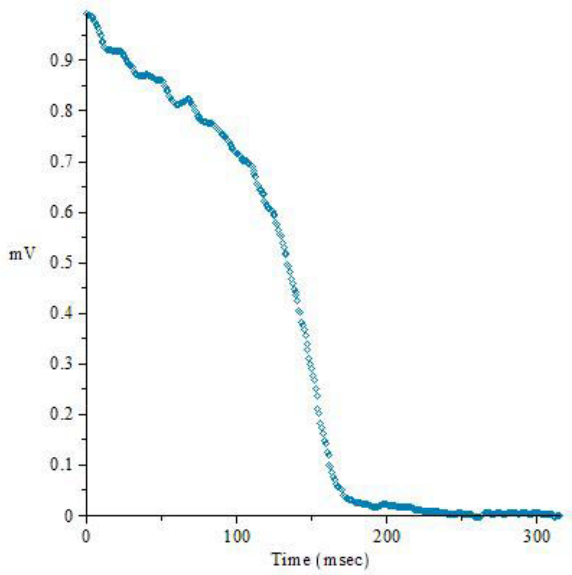

Figure 10: Portion of cMc data set from Figure 6 that was used to build our model. The membrane voltage has been rescaled to be between 0 and 1. Additionally, the data points before the peak point of depolarization have been ignored. These points are ignored because of the difficulty in fitting the few points that compose the depolarization and because our interest is modeling the repolarization of the action potential where the interaction between fast and slow ion interactions occur.

$$U(t) = \frac{1 + aB_2e^{-pt}}{1 + B_2e^{-pt} + C_2e^{qt}} \tag{15}$$

where $B_2 = B_1e^{\frac{x}{\sqrt{2}}(a-1)}$, $C_2 = C_1e^{\frac{-x}{\sqrt{2}}}$, $p = (\frac{1}{2} - \frac{a^2}{2})$, and $q = (a - \frac{1}{2})$.

In order to estimate the parameter q, we set $B_2 = 0$, giving us:

$$U(t) = \frac{1}{1 + C_2e^{qt}} \tag{16}$$

We can now fit a portion of the action potential with this equation to estimate C_2 and q, but first we want to make a substitution for C_2. When we initially ran a non-linear regression fit on the full action potential we saw that the estimates for B_2 and C_2 were very large with magnitudes of 10^{26} and 10^{24}, respectively. In the above equation, C_2 is in units of voltage and independent of time. However, C_2 is not independent of q. Therefore, we introduce the following substitution $C_2 = e^{-qg}$. By writing C_2 as an exponential, we get parameter values that are more physiologically reasonable. Setting $B_2 = 0$, U is reduced to

$$U(t) = \frac{1}{1 + e^{q(t-g)}} \tag{17}$$

Next, notice in Figure 10 that as t goes to infinity, the voltage recording goes to zero. Correspondingly, in Equation 17, we want q such that as t goes to infinity, $U(t)$ goes to zero. Thus, we have

$$\lim_{t\to\infty} U(t) = \lim_{t\to\infty} \frac{1}{1 + e^{qt}e^{q(-g)}} = 0 \tag{18}$$

only if $q > 0$. Physiologically, we can now use Equation 17 to model the portion of the action potential that tends to zero as time goes to infinity. These are the data points, seen in Phase 3 of Figure 2, which directly follow the plateau phase.

After rearranging and taking the natural logarithm of both sides, we obtain a linear equation where $y = U(t)$:

$$\ln \frac{1 - y}{y} = qt - qg \tag{19}$$

From this equation, we use a linear regression fit on the data points following the plateau to obtain a unique estimation of the parameters q and g. We use our unique estimates of q and g to find the other parameters using non-linear estimation. Additionally, this linear analysis gives us an additional check when evaluating our model: if our estimate of q is not positive, then our model is wrong.

Before running a non-linear estimation, we return to Equation 15. We choose to make a substitution for B_2 similar to the one we made for C_2. Again, B_2 is not dependent on time, but does depend on the value of p. Letting $B_2 = e^{ph}$, where h is a constant parameter, we have

$$U(t) = \frac{1 + ae^{ph}e^{-pt}}{1 + e^{-p(t-h)} + e^{q(t-g)}} \tag{20}$$

Notice that we do not combine the two exponentials in the numerator of Equation 20. Rather, we now introduce a small perturbation of p in order to encompass both the fast and slow ion currents in our model. Our perturbation is $r = p + \delta$ where δ is a small number. This is a singular perturbation approach; please see the Appendix for justification of this perturbation parameter. This gives us the solution $U(t)$ that we use to model cardiac action potentials via non-linear estimation:

$$U(t) = \frac{1 + e^{-r(t-f)}}{1 + e^{-p(t-h)} + e^{q(t-g)}} \tag{21}$$

We use *Maple 14* to estimate q and g by linear estimation and to estimate our other parameters by non-linear regression. We give initial estimates for p and h, along with the initial estimates of q and g from the linear estimation, to run a weighted non-linear regression to estimate r, f, p, h, q, and, g in our model, Equation 21. We use weights in our estimation because of the sharp turn in myocyte action potentials. The weights enable us to dictate which data points have the most influence when running the non-linear regression to build our model. We use the following weight sequence:

$$weights = (val)^n \tag{22}$$

where val is a number between 0 and 1 and $n = 1, 2, ..., z$ where z is the number of data points for the action potential. Thus, the earlier data points

have more influence in building the model then later data points of an action potential.

6.3 Evaluation of Model

We evaluate our model for each cardiac action potential by analyzing the residuals. Specifically, we examine four aspects of the residuals: normality, residual sum of squares, residual mean square, and residual standard deviation.

The first aspect we check when evaluating whether our model is good or not is the distribution of the model's residuals by examining a histogram of the residuals. We want a normal distribution centered around zero. That is, we want most of our residuals to be zero or very close to zero, and we want to have an equal number of positive and negative residuals. A residual, e, is a measure of the distance between a model's predicted value and the actual value of the data. Mathematically, a residual is defined as $e = y - \hat{y}$, where y is the actual value and $\hat{y}$ is the predicted value. Clearly, the more residuals which have a value of zero, the better our model is at fitting the action potential. Similarly, if the histogram is not skewed, then our model does not underpredict or overpredict our data.

Second, we examine the residual sum of squares, $\sum e^2$. This gives us another measure of the variability between the model's predicted values and the actual data. By squaring the residuals, we are summing positive values and thus obtain a measure of the difference between predicted and actual values. Obviously, we want the residual sum of squares to be as small as possible. The residual sum of squares is particularly useful in comparing the predictions of a model when we change parameter values and/or the weights.

Third, we consider the residual mean square:

$$RMS = \frac{\sum e^2}{df} \tag{23}$$

where df is the residual degrees of freedom of the model. Mathematically, $df = n - p$, where n is the number of data points in the set and p is the number of parameters in the model, which in our case is six. For our purposes, the

residual mean square is useful for comparing our model's predictability from one data set to another.

Finally, we examine the standard deviation of the residuals, which is denoted s

$$s = \sqrt{\frac{\sum e^2}{df}} = \sqrt{RMS} \tag{24}$$

s is a goodness-of-fit test and is used to evaluate which model is better at fitting the data. The best model has the smallest value of s. Again, we can use s to see which weights and parameter values optimize our model of a myocyte action potential.

7 Results

We first show the results of our model when applied to the guinea pig ventricular myocyte AP in Figure 5. The following initial values were used to model the action potential in *Maple 14*: $g = 192.0, q = 0.049, p = 0.01$, and $h = -20$. Table 2 gives the value of each parameter when a different val is used in the weighted non-linear regression.

Table 2: Guinea Pig Ventricular Myocyte							
Val	f	g	h	p	q	r	1.96·RSD
0.975	-95645.3	2679.5	29608.0	-6.0E-02	1.1E-03	2.6E-01	1.9E-02
0.98	-55.9	200.3	230.9	-1.1E-01	1.0E-01	4.6E-02	1.6E-03
0.985	15.3	189.6	125.8	7.3E-04	6.4E-02	5.2E-03	4.4E-03
1	-394.8	203.4	211.1	-1.3E-02	1.6E-01	8.6E-03	2.4E-02

Note our model had a hard time obtaining a fit when $val = 0.99$ and when $val = 0.995$. Also, the $1.96 \cdot RSD$ gives a rough confidence interval for each parameter with the given val.

Table 3 gives the Residual Sum of Squares (RSS), the Residual Mean Square (RMS), the Residual Standard Deviation (RSD), and the Degrees of Freedom (df) of our model for each val.

Table 3: G. Pig Vent. Myocyte				
Val	RSS	RMS	RSD	df
0.975	3.01E-02	9.58E-05	9.79E-03	314
0.98	2.02E-04	6.44E-07	8.03E-04	314
0.985	1.55E-03	4.93E-06	2.22E-03	314
1	4.64E-02	1.48E-04	1.22E-02	314

Tables 4 and 5 show the parameter estimates and residual measures for the single pig myocyte data, shown in Figure 6. Our initial values were $g = 133.8, q = 0.047, p = 0.01$, and $h = -20$.

Table 4: Single Pig Myocyte							
Val	f	g	h	p	q	r	1.96·RSD
0.975	869.4	69.9	362.6	-1.9E-03	8.4E-03	1.4E-05	6.4E-03
0.98	-34.1	143.7	168.5	-1.4E-02	9.8E-02	7.1E-02	3.8E-03
0.985	15.1	134.8	37.5	5.9E-03	6.4E-02	1.3E-02	5.7E-03
0.99	-32.7	144.2	164.8	-1.5E-02	1.0E-01	7.5E-02	5.6E-03
0.995	9.0	136.4	-37.5	-2.0E-03	9.0E-02	3.9E-03	1.1E-02
1	-63.8	136.1	-1.2	-4.6E-03	9.6E-02	7.2E-04	2.0E-02

Table 5: Single Pig Myocyte				
Val	RSS	RMS	RSD	df
0.975	3.71E-03	1.08E-05	3.28E-03	344
0.98	1.31E-03	3.79E-06	1.95E-03	344
0.985	2.94E-03	8.55E-06	2.92E-03	344
0.99	2.81E-03	8.16E-06	2.86E-03	344
0.995	1.10E-02	3.19E-05	5.65E-03	344
1	3.66E-02	1.06E-04	1.03E-02	344

Tables 6 and 7 give the parameter estimates and residual measures for the simulated purkinje fiber data, seen in Figure 7. Our initial values were $g = 340.3, q = 0.016, p = 0.01$, and $h = -20$.

Table 6: Simulated Purkinje Fiber							
Val	f	g	h	p	q	r	1.96·RSD
0.97	-70.9	313.2	-222.0	3.7E-03	4.1E-02	1.1E-02	2.6E-03
0.975	-84.2	314.2	-361.9	3.0E-03	3.8E-02	1.3E-02	2.8E-03
0.98	83.4	311.0	102.7	1.2E-02	2.9E-02	1.5E-02	2.8E-03
0.985	-76.2	314.5	-301.0	3.6E-03	3.4E-02	1.4E-02	3.5E-03
1	42.0	137.1	39.8	-6.2E-02	9.6E-02	-6.3E-02	1.4E-02

Table 7: Sim. Purkinje Fiber				
Val	RSS	RMS	RSD	df
0.97	6.07E-04	1.70E-06	1.31E-03	354
0.975	7.48E-04	2.11E-06	1.45E-03	354
0.98	7.03E-04	1.99E-06	1.41E-03	354
0.985	1.12E-03	3.16E-06	1.78E-03	354
1	1.90E-02	5.37E-05	7.33E-03	354

Note our model again had a hard time obtaining a fit for the Simulated Purkinje Fiber data when $val = 0.99$ and when $val = 0.995$.

Tables 8 and 9 show the parameter estimates and residual measures for the healthy canine myocyte data, displayed in Figure 8. Our initial values were $g = 236.0, q = 0.049, p = 0.01$, and $h = -20$.

Table 8: Healthy Canine Myocyte							
Val	f	g	h	p	q	r	1.96·RSD
0.975	26867.8	-507.1	27691.7	-2.4E-01	-8.7E-02	-2.4E-01	3.8E-02
0.98	89.5	216.5	78.3	-2.2E-02	1.1E-01	-2.0E-02	2.3E-03
0.99	134.9	238.7	102.2	-1.4E-02	1.3E-01	-1.1E-02	4.7E-03
0.995	489.1	156.8	551.0	1.7E-02	5.4E-02	1.9E-02	3.1E-02

Table 9: Healthy Canine Myo.				
Val	RSS	RMS	RSD	df
0.975	7.11E-02	3.67E-04	1.91E-02	194
0.98	2.58E-04	1.33E-06	1.15E-03	194
0.99	1.14E-03	5.86E-06	2.42E-03	194
0.995	4.94E-02	2.55E-04	1.60E-02	194

We note that our model had difficulty obtaining a fit for the healthy canine myocyte when $val = 0.985$ and when $val = 1$.

Finally, we show the parameter estimates and residual measures for a failing canine myocyte. Table 10 and 11 show the results when the initial estimates of q and g were obtained with a linear fit of the data points 340-355 while Table 12 and 13 display the results when q and g are estimated with a linear fit of the data points 355-370.

Table 10: Failing Canine Myocyte (340-355)							
Val	f	g	h	p	q	r	1.96·RSD
0.985	107.5	612.6	181.3	3.0E-03	6.7E-03	5.1E-03	2.4E-03
0.99	-35.3	569.7	-260.1	3.9E-04	4.4E-02	3.1E-03	3.8E-03
0.995	12.3	577.4	-316.5	-1.4E-04	8.4E-02	2.0E-03	8.4E-03

Table 11: F. Can. Myo. (340-355)				
Val	RSS	RMS	RSD	df
0.985	6.02E-04	1.49E-06	1.22E-03	404
0.99	1.52E-03	3.77E-06	1.94E-03	404
0.995	7.49E-03	1.85E-05	4.31E-03	404

Table 12: Failing Canine Myocyte (355-370)							
Val	f	g	h	p	q	r	1.96·RSD
0.985	-37.5	597.3	-126.1	1.3E-03	9.2E-03	4.3E-03	2.4E-03
0.99	-24.6	570.4	-169.0	4.0E-04	4.4E-02	3.1E-03	3.8E-03
0.995	-4.9	577.6	-58.5	-1.8E-04	8.5E-02	2.0E-03	8.4E-03

Table 13: F. Can. Myo. (355-370)				
Val	RSS	RMS	RSD	df
0.985	5.99E-04	1.48E-06	1.22E-03	404
0.99	1.53E-03	3.79E-06	1.95E-03	404
0.995	7.48E-03	1.85E-05	4.30E-03	404

8 Discussion

As seen in the residual tables, our model does a good job fitting an action potential in a variety of cardiac cell types. We now show a plot of actual action potentials versus the fit from our model for each data set along with a histogram of the residuals. Each figure below is based on the model with Val set to the number that gives the lowest RSS, RMS, and RSD. For the most part, $Val = 0.98$ gave the best fit but there were a couple of exceptions, which are noted in the figures below.

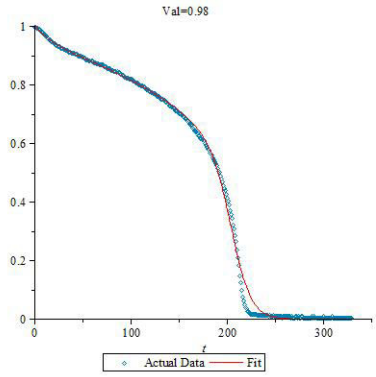

Figure 11: Action potential from a single ventricular myocyte in a guinea pig.

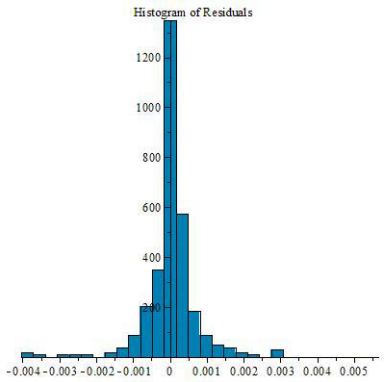

Figure 12: The fit is from when $Val = 0.98$ in our weighted non-linear regression model.

Note, although the residual measures were smaller for $Val = 0.985$ in the failing canine data set, the weights were insufficient in making the fit drop back down to the resting potential. Hence, we show the results for $Val = 0.99$ in Figures 19 and 20.

The plots of actual versus fits indicate that our model does a good job of describing single myocyte action potentials. Additionally, the histograms of residuals all show a fairly normal distribution with no skewness. This is significant because if the residuals had been skewed, then our model would be

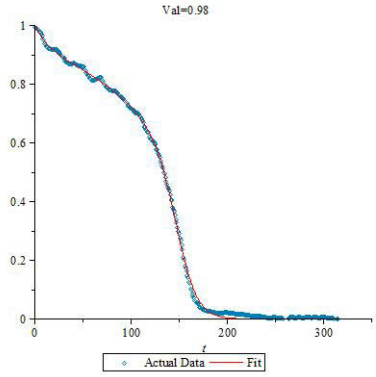

Figure 13: Action potential from a single ventricular myocyte in a pig.

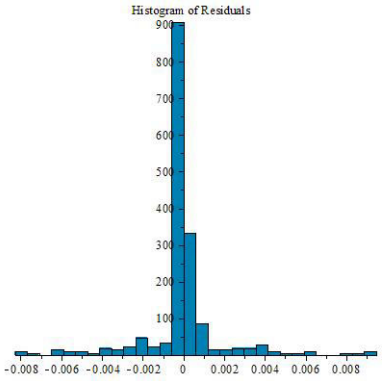

Figure 14: The fit is from when $Val = 0.98$ in our weighted non-linear regression model.

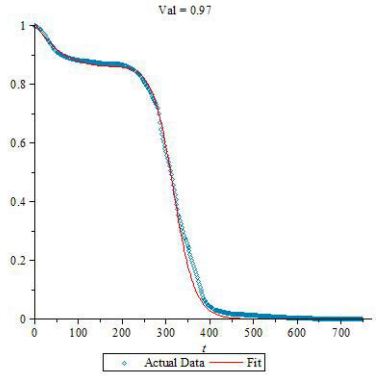

Figure 15: Simulated action potential from Noble's model of purkinje fibers.

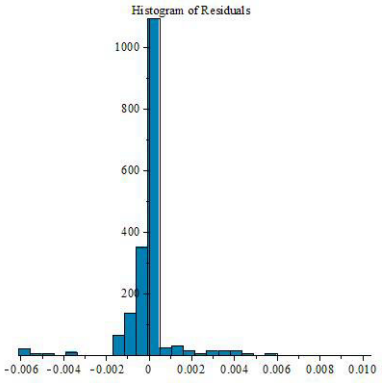

Figure 16: The fit is from when $Val = 0.97$ in our weighted non-linear regression model.

overfitting or underfitting the action potential. These two facts, along with the low values for RSS, RMS, and RSD, corroborate that our model does a good job in describing the variability seen in myocyte action potentials.

But does our singular perturbation assumption hold in all of our models: that is, is δ a small number, where $\delta = r - p$? In order to evaluate this, we calculate the relative difference between r and p for the best Val in each data set. The relative differences are shown in Table 14. The lower the relative

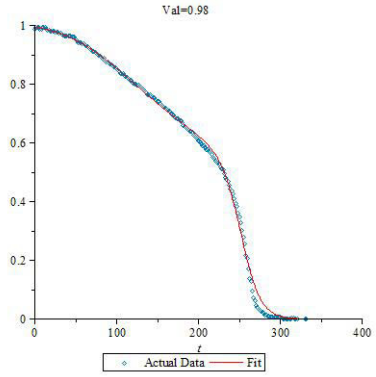

Figure 17: Action potential from a healthy canine myocyte.

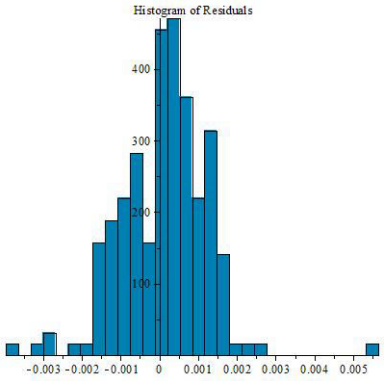

Figure 18: The fit is from when $Val = 0.98$ in our weighted non-linear regression model.

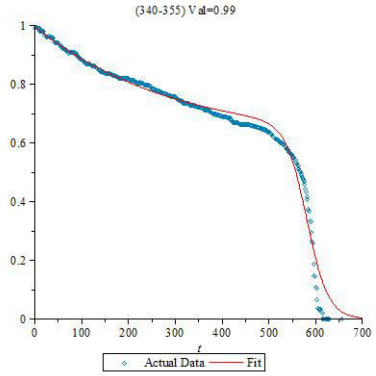

Figure 19: Action potential from a failing canine myocyte.

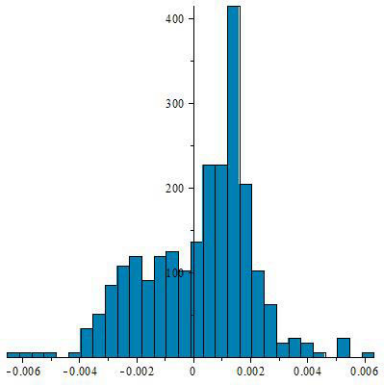

Figure 20: The fit is from when $Val = 0.99$ in our weighted non-linear regression model.

difference, the closer r is to p, or equivalently, the smaller the relative value of δ. For example, a relative difference of 2.5, means that r or p is 2.5 times greater than the other. Recall, that we want δ to be small.

Table 14: Relative Differences of $\delta = p - r$

AP	Spig	Gpig	Purkinje	Healthy	Failing (340-355)	Failing (355-370)
Rel. Diff.	5.908	3.469	2.049	0.118	6.949	6.696

The relative difference is lowest for the healthy canine myocyte. The relative differences for the simulated purkinje fiber and guinea pig ventricular myocyte are also reasonably small. Therefore, we can justify our perturbation assumption that p is close to r for these three data sets. However, we cannot justify this assumption with the pig myocyte data set or the failing canine data sets. Our research hypothesis is: if a cardiac action potential can be modeled by a singular perturbation of the Fitzhugh-Nagumo PDE, then our model will be confirmed if a) p is close to r and b) the model is good statistically, that is, the model has small RSS, RMS, and RSD values. The contrapositive of our hypothesis is: If our model is good statistically but p is not close to r, then the action potential is not a singularly perturbed Fitzhugh-Nagumo action potential. Following this logic, we can conclude that failing myocytes do not operate as singularly perturbed Fitzhugh-Nagumo action potentials even though our model does a good job fitting the action potential. Thus, our model could be used to study healthy and failing myocytes in order to determine which parameter values cause an action potential to be 'failing.'

Thus, we see that the singular perturbation step is crucial in order for us to be able to model the full myocyte action potential. Without our perturbation, $r = p + \delta$, we are only able to describe the fast ion currents of the action potential. However, the perturbation enables us to encompass the slow ion currents into our model. The importance of perturbing the known solution to the Fitzhugh-Nagumo PDE with δ is clearly seen when we plot the actual versus fits of our perturbed model beside a non-perturbed model in Figures 21 and 22.

Notice the scale on the y-axis of Figure 22. Because the scale is 10^4 for the fit, the actual action potential looks like a straight line with a membrane potential equal to zero. Without the perturbation, we cannot model the full action potential. Physiologically, this is because the slow ion currents direct repolarization, and if we do not model the slow ion currents, we cannot accurately describe the action potential.

While we were able to build a good model of myocyte action potentials, there are a few topics that could be explored in more depth. First, a better understanding of the physiological significance of our parameters is desirable. This would allow us to draw better conclusions about the interactions

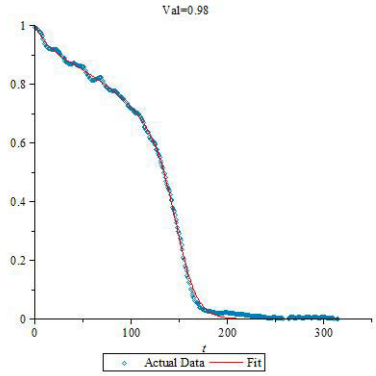

Figure 21: Perturbed model for a single ventricular myocyte action potential in a pig.

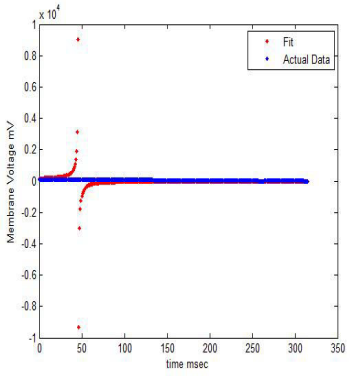

Figure 22: Non-perturbed model for a single ventricular myocyte action potential in a pig.

between ions that are occurring at the end of the plateau phase as well as at other locations in the action potential. Second, sensitivity testing could be done on the parameters to establish parameter independence and dependence. Until then our confidence intervals reported in our results only hold for products of parameters. Third, more work could be done establishing what changes in parameters lead to failure in a myocyte. In particular, it would be interesting to develop a sequence of myocytes for which an action potential is propagated down and determine at what point a myocyte in the sequence becomes failing. That is, when does the myocyte fail to produce a singular perturbed Fitzhugh-Nagumo action potential.

9 Conclusion

Overall, we were able to show that a myocyte action potential can be modeled by applying a singular perturbation approach to the Fitzhugh-Nagumo PDE. The singular perturbation is necessary to encompass the slow ion currents which are responsible for part of repolarization. This model was successful in describing four different types of cardiac action potentials. A model of this type has much potential in the medical field. It can be used to better understand the interaction of ions responsible for producing an action potential. In addition, a model such as this could be used to study what causes a myocyte to have a 'failing' action potential, which may lead to an arrhythmia.

Finally, the method that we applied in building our model may have value in modeling other types of excitable cells.

10 Appendix

10.1 Singular Perturbation Theory

We begin with some notation from perturbation theory. Suppose we have a problem $P_\epsilon(y) = 0$ which depends on the small parameter ϵ. We will denote its solution by y_ϵ. Correspondingly, the limiting problem, when $\epsilon = 0$, $P_0(y)$ has the solution y_0. Then, P_ϵ is a *regular* perturbation if

$$\lim_{\epsilon \to 0} y_\epsilon = y_0 \tag{25}$$

Otherwise, P_ϵ is a *singular* perturbation [16].

In brief, perturbation theory is applied to a problem that does not have an exact solution but is close to an auxiliary problem that does have an exact solution. Singular perturbation theory allows the use of an exact solution even when the exact solution is NOT a limiting solution. The original problem should have a solution that is close to the solution of the auxiliary problem [17]. In our case, we know the solution to the fast part of the cardiac action potential when the myocyte is depolarized by the inward flow of Na^+ ions. That is, our auxiliary problem is the Fitzhugh-Nagumo PDE. The solution to the Fitzhugh-Nagumo equation that we chose to work with is given in Equation 27. In order to find a solution to the PDE describing the entire cardiac action potential, we need to perturb the Fitzhugh-Nagumo solution. In our methods section, we perturbed the solution to the Fitzhugh-Nagumo PDE such that it described a myocyte action potential. We now justify this approach to modeling cardiac action potentials.

Recall that the Fitzhugh-Nagumo PDE is given by:

$$\frac{\partial u}{\partial t} = \frac{\partial^2 u}{\partial x^2} + u(1-u)(a-u) \tag{26}$$

One known solution for the Fitzhugh-Nagumo PDE is

$$U(x,t) = \frac{Ae^{z_1} + Be^{z_2}}{Ae^{z_1} + Ce^{z_2} + D} \tag{27}$$

where U is the voltage at position x and time t, $z_1 = \frac{x}{\sqrt{2}} + (\frac{1}{2} - a)t$, $z_2 = \frac{ax}{\sqrt{2}} + a(\frac{a}{2} - 1)t$, and A, B, and C are arbitrary constants.

We begin by noting the Fitzhugh-Nagumo fast (ν) and slow (ω) PDEs [1]:

$$\epsilon \frac{\partial \nu}{\partial t} = \epsilon^2 \frac{\partial^2 \nu}{\partial x^2} + \nu(1-\nu)(a-\nu) - \omega \tag{28}$$

$$\frac{\partial \omega}{\partial t} = \nu - \gamma\omega - \nu_0 \tag{29}$$

where ν_0 is the resting membrane potential. We will let $\nu_0 = 0$ for the rest of our work.

We next find the two outer solutions by setting $\epsilon = 0$ in the Fitzhugh-Nagumo fast and slow equations, Equations 28 and 29. Hence, our **outer solutions** are:

$$v(1-v)(a-v) - w = 0 \tag{30}$$

$$\frac{\partial w}{\partial t} = v - \gamma w \tag{31}$$

We then introduce a substitution term, ξ, to find the two inner solutions

$$\xi = \frac{x - y(t)}{\epsilon} \tag{32}$$

Note, as ϵ approaches zero, ξ approaches infinity. In general for perturbation theory, we would want our substitution to be on a different time scale. Hence, we define ξ to be:

$$\xi = \frac{x - y(\tau)}{\epsilon} \tag{33}$$

We also define a new polynomial $v(\xi, \tau)$. We let v be our polynomial in Equation 28, and we make our ξ substitution for the $\frac{\partial^2}{\partial x^2}$ term:

$$\frac{\partial v}{\partial x} = \frac{\partial v}{\partial \xi}\frac{\partial \xi}{\partial x} = \frac{1}{\epsilon}\frac{\partial v}{\partial \xi} \tag{34}$$

$$\frac{\partial^2 v}{\partial x^2} = \frac{1}{\epsilon}\frac{\partial v_\xi}{\partial \xi}\frac{\partial \xi}{\partial x} = \frac{1}{\epsilon^2}\frac{\partial^2 v}{\partial \xi^2} \tag{35}$$

where $v_\xi = \frac{\partial v}{\partial \xi}$.

We now make the ξ substitution for the $\frac{\partial}{\partial t}$ term in Equation 28:

$$\frac{\partial v}{\partial t} = \frac{\partial v}{\partial \xi}\frac{\partial \xi}{\partial t} + \frac{\partial v}{\partial \tau}\frac{\partial \tau}{\partial t} = \frac{\partial v}{\partial \xi}\frac{-y'(\tau)}{\epsilon} + \frac{\partial v}{\partial \tau} \tag{36}$$

since in our case $t = \tau$. This is because the time is the same for both. [1]

Plugging our two substitutions into Equation 28, gives

$$\epsilon\left(\frac{\partial v}{\partial \xi}\frac{-y'(\tau)}{\epsilon} + \frac{\partial v}{\partial \tau}\right) = \frac{\partial^2 v}{\partial \xi^2} + \nu(1-\nu)(a-\nu) - \omega \tag{37}$$

Multiplying through and rearranging Equation 37, we obtain our **first inner solution**:

$$\frac{\partial^2 v}{\partial \xi^2} + y'(t)\frac{\partial v}{\partial \xi} + v(1-v)(a-v) - \omega = \epsilon\frac{\partial v}{\partial \tau} \tag{38}$$

To get the second inner equation, we make a similar ξ substitution in the slow Fitzhugh-Nagumo PDE, Equation 29, letting $w(\xi, \tau)$ be our polynomial:

$$\frac{\partial w}{\partial t} = \frac{\partial w}{\partial \xi}\frac{-y'(\tau)}{\epsilon} + \frac{\partial w}{\partial \tau} \tag{39}$$

We apply our substitution to Equation 29, multiply through, and rearrange terms to obtain the **second inner solution**:

$$-y'(\tau)\frac{\partial w}{\partial \xi} = \epsilon(v - \gamma w) - \epsilon\frac{\partial w}{\partial \tau} \tag{40}$$

In our ξ substitution, we assume $\xi \to \infty$ quicker than $\epsilon \to 0$. Thus, we assume $\epsilon = 0$ in our two inner equations *because why* to obtain:

$$v_{\xi\xi} + y'(t)v_\xi + v(1-v)(a-v) - w = 0 \tag{41}$$

$$-y'(t)w_\xi = 0 \tag{42}$$

[1] In special relativity, t is time relative to a fixed observer and τ is time relative to a moving observer. But in our case, the time is the same for both observers.

where $v_{\xi\xi} = \frac{\partial^2 v}{\partial \xi^2}$, $v_\xi = \frac{\partial v}{\partial \xi}$, and $w_\xi = \frac{\partial w}{\partial \xi}$

But, we know $y'(t) \neq 0$. Hence in the slow outer solution, we must have $w_\xi = 0$. That is, w is not a function of ξ and thus

$$w = w(\tau) \tag{43}$$

We can now examine the matching condition. The matching condition compares the limit of the inner solution as $\xi \to \infty$ to the limit of the outer solution as $\epsilon \to 0$. We will compare the inner, Equation 41, and outer, Equation 30, solutions of the fast Fitzhugh-Nagumo PDE, Equation 28.

$$\lim_{\xi \to \pm\infty} v_{\xi\xi} + y'(\tau)v_\xi + v(1-v)(a-v) - w = \lim_{\epsilon \to 0} \epsilon \frac{\partial v}{\partial t} + \epsilon^2 \frac{\partial^2 v}{\partial x^2} + v(1-v)(a-v) - w \tag{44}$$

Note that the $v_{\xi\xi}$ and v_ξ terms go to zero as $\xi \to \infty$. Hence, our inner and outer solutions match.

Now, we return to our specific solution of the Fitzhugh-Nagumo PDE, Equation 27. We let $U(x,t)$ be the polynomial ν in Equations 28 and 29. Our inner and outer solutions will be the same as the ones found for the polynomial v. The first inner solution with $\epsilon = 0$ gives us:

$$U_{\xi\xi} + y'(t)U_\xi + U(1-U)(a-U) = w = f(\tau) \tag{45}$$

since by Equation 43, w only depends on τ.

Thus, $U = U(\xi, y'(\tau), w(\tau), A, B)$, and when we plug U into the slow Fitzhugh-Nagumo PDE, we see that U depends on five parameters. However, y and w only depend on τ. We can get rid of two more parameters by the matching condition: one as $\xi \to +\infty$ and another as $\xi \to -\infty$. Thus, ϵ depends on only one parameter, which is what we want. Also, note that our matching condition shows that the parameters of the fast and slow PDEs are not independent.

To summarize where we are at this point, we have a solution to the Fitzhugh-Nagumo PDE, Equation 26. That is, we can model the depolarization of a cardiac myocyte. Our goal is to obtain a solution for the fast and

slow Fitzhugh-Nagumo PDEs, Equations 28 and 29, so that we can model the entire myocyte action potential.

Our next step is to let

$$v(x,t,\epsilon) = \sum_{j=0}^{\infty} v_j(x,t)\epsilon^j \tag{46}$$

$$w(x,t,\epsilon) = \sum_{j=0}^{\infty} w_j(x,t)\epsilon^j \tag{47}$$

where $v_0(x,t) = U(\epsilon^{-1}x, \epsilon^{-1}t)$ and $w_0(x,t) = 0$. We want to find $v_1(x,t)$. We do not worry about higher orders of v because of the Perturbation Assumption: that is, we are assuming ϵ is so small that $v_j(x,t)\epsilon^j$ is negligible for $j > 1$. Note that higher order ϵ would be in our residuals.

Next, we substitute v_1 and w_1 into the fast and slow Fitzhugh-Nagumo PDEs.

$$\begin{aligned} \epsilon\frac{\partial}{\partial t}(v_0 + \epsilon v_1) &= \epsilon^2\frac{\partial^2}{\partial x^2}(v_0 + \epsilon v_1) \\ &+ (v_0 + \epsilon v_1)[1 - (v_0 + \epsilon v_1)][a - (v_0 + \epsilon v_1)] - \epsilon w_1 \end{aligned} \tag{48}$$

$$\frac{\partial}{\partial t}\epsilon w_1 = (v_0 + \epsilon v_1) - \gamma\epsilon w_1 \tag{49}$$

These equations can be simplified:

$$\epsilon^2\frac{\partial v_1}{\partial t} = \epsilon^3\frac{\partial^2 v_1}{\partial x^2} + v_1(3v_0^2 - 2v_0 - 2v_0 a + a)\epsilon - \epsilon w_1 \tag{50}$$

$$\frac{\partial}{\partial t}w_1 = v_1 - \gamma w_1 \tag{51}$$

Notice when expanding Equation 48 to obtain Equation 50 that

$$\epsilon\frac{\partial v_0}{\partial t} = \epsilon^2\frac{\partial^2 v_0}{\partial x^2} + v_0(1 - v_0)(a - v_0) \tag{52}$$

Also, note that we ignore terms of v_1 with a power higher than 1.

More importantly, Equation 50 is a linear PDE; hence, we can solve it to obtain our solution.

We can now justify our model of cardiac action potentials. We know Equation 27 is a solution to Equation 26 in the form of

$$v(x,t) = \frac{1 + D(t)e^{z_2 - z_1}}{1 + Be^{z_2 - z_1} + Ce^{-z_1}} \tag{53}$$

where we first multiplied $U(x,t)$ by $\frac{\frac{1}{A}e^{-z_1}}{\frac{1}{A}e^{-z_1}} = 1$ and where $D = aB$. That is,$v(x,t) = U(x,t,D(t))$. Thus, $\frac{\partial^2 v}{\partial x^2} = \frac{\partial^2 u}{\partial x^2}$, and letting $t = \tau$, we have $v(x,t) = U(x,\tau,D(\tau))$. We can now apply the chain rule to expand $\frac{\partial v}{\partial t}$

$$\frac{\partial v}{\partial t} = \frac{\partial u}{\partial \tau}\frac{\partial \tau}{\partial t} + \frac{\partial u}{\partial D}\frac{\partial D}{\partial t} \tag{54}$$

$$\frac{\partial v}{\partial t} = \frac{\partial u}{\partial \tau} + \frac{\partial u}{\partial D}\frac{\partial D}{\partial t} \tag{55}$$

Since

$$\frac{\partial v}{\partial t} = \frac{\partial^2 v}{\partial x^2} + v(1-v)(a-v) \tag{56}$$

a solution to

$$\frac{\partial U}{\partial t} = \frac{\partial^2 U}{\partial x^2} + U(1-U)(a-U) - w \tag{57}$$

with $U = u(x,t,D(t))$ will satisfy

$$\frac{\partial v}{\partial t} + \frac{\partial U}{\partial D}\frac{\partial D}{\partial t} = \frac{\partial^2 U}{\partial x^2} + U(1-U)(a-U) - w \tag{58}$$

Recalling that $\frac{\partial^2 v}{\partial x^2} = \frac{\partial^2 u}{\partial x^2}$ and $v(x,t) = u(x,t,D(t))$, we use Equation 56 to obtain:

$$\frac{\partial U}{\partial D}\frac{\partial D}{\partial t} = -w \tag{59}$$

We now introduce our perturbation to the PDE by setting $D(t) = Ee^{-\delta t}$, where E is an arbitrary constant. Taking the derivative of D with respect to time, we find

$$D'(t) = Ee^{-\delta t}(-\delta) = -\delta D \tag{60}$$

Substituting this result into Equation 59, we have

$$w = \delta \frac{\partial U}{\partial D} D \tag{61}$$

We next substitute for w in the slow Fitzhugh-Nagumo PDE

$$\begin{aligned} \frac{\partial w}{\partial t} &= U - \gamma w & (62) \\ \delta \frac{\partial}{\partial t}\left(\frac{\partial U}{\partial D} D\right) &= U(x,t,D(t)) - \gamma\delta \frac{\partial U}{\partial D} D & (63) \end{aligned}$$

Now, we just need to find a solution to Equation 63. But Equation 63 is a linear ODE, which can always be solved! The solution to this ODE is

$$\delta \frac{\partial U}{\partial D} D = K + \int_0^t e^{-\gamma(t-\tau)} U(x,\tau; D(\tau))\, d\tau \tag{64}$$

Next, we need to estimate the parameter K. Recall our matching condition:

$$\lim_{\xi \to \pm\infty} U(\xi, t) = \lim_{\epsilon \to 0} U(x, t, \epsilon) \tag{65}$$

As ϵ goes to 0 the limit on the right side goes to K. However, as ξ approaches ∞, the Fitzhugh-Nagumo PDE produces an action potential before returning to the resting potential, which we set to be zero when we let $v_0 = 0$ in Equation 29. Therefore, the value of K is determined by the matching condition.

Since all of the parameters in our model can be accounted for or can be estimated, we have justified the form of our model. That is, we have justified our perturbation of p being $r = p + \delta$.

10.2 Computer Code

The following *Maple 14* code verifies that Equation 13 is indeed a solution of the Fitzhugh Nagumo PDE, Equation 12.

```
# F-N Solution:
z1:=(sqrt(2)/2)*x+(1/2-a)*t:
z2:=(sqrt(2)/2)*a*x+a*((1/2)*a-1)*t:
w:=(A*exp(z1)+a*B*exp(z2))/(A*exp(z1)+B*exp(z2)+C):
Partial_t:=diff(w,t):
SecondPartial_x:=diff(w,x,x):
Left_Side:=Partial_t-SecondPartial_x:
Left_Side_Simp:=simplify(Left_Side):
Right_Side:=-w*(1-w)*(a-w):
Right_Side1:=-a*w+w^2+a*w^2-w^3:
Right_Side1_Simp:=simplify(Right_Side1):
Check:=Left_Side_Simp-Right_Side1_Simp:
simplify(Check):
```

The following *Maple 14* code was used to get initial estimates of q and g and then to run a weighted non-linear regression fit for our model.

```
tran := 154..165:
TT := Time[tran]:
VV := Volt[tran]:
pVV := map( x-> ln( (1-x)/x ), VV):
ScatterPlot( Time, map( x -> ln( (1-x)/x ), Volt) ):
LogPlot:=ScatterPlot( TT, pVV ):LogPlot:
LinFit:=LinearFit([1,t],TT,pVV,t, output=solutionmodule):
params := LinFit:-Results(parametervalues):
wghts := [seq( (0.98)^n, n=1..200 ) ]:
y := (1+exp(-r*(t-f))) / (1+exp(-p*(t-h))+exp(q*(t-g))):
yFitmodule:=Fit( y, Time[1..200], Volt[1..200], t, weights = wghts ,
   initialvalues = [ g=abs(params[1]/params[2]), q=params[2], p=0.01, h=-20 ] ,
   output=solutionmodule):
```

References

[1] Keener, J., Sneyd, J. (2004). *Mathematical Physiology.* New York: Springer Science.

[2] "About Arrhymia." (2011). American Heart Association. Retrieved January 11, 2011 from `http://www.heart.org/HEARTORG/Conditions/Arrhythmia/AboutArrhythmia/About-Arrhythmia_UCM_002010_Article.jsp`.

[3] "Atrial Fibrillation" (2011). American Heart Association. Retrieved January 11, 2011 from `http://www.americanheart.org/presenter.jhtml?identifier=4451`.

[4] Huikuri, Heikki V., Agustin Castellanos, and Robert J. Myenburg (2001). "Sudden Death Due to Cardiac Arrhythmias." *New England Journal of Medicine.* Vol. 345, No. 20. 2001. 1473-1482.

[5] Noble, Denis (2007). "From the Hodgkin-Huxley Axon to the Virtual Heart." *Journal of Physiology.* Vol. 580, No.1, 15-22.

[6] Fischer, Teresa G. (2011) "Anatomy and Physiology I: Lecture Notes." Retrieved January 12, 2011 from `http://faculty.irsc.edu/FACULTY/TFischer/AP1/resting%20membrane%20potential2.jpg`.

[7] Wilk, Malgosia (2007). "Physiology of Excitable Cells." Retrieved January 12, 2011 from `http://www.uta.edu/biology/wilk/classnotes/cellphys/excitable%20cells.pdf`.

[8] Hinch, Robert (2002). "An analytical study of the physiology and pathology of the propagation of cardiac action potentials." *Progress in Biophysics and Molecular Biology.* Vol. 78. 2002. 45-81.

[9] Klabunde, Richard E. (2008). "Non-Pacemaker Action Potentials." *Cardiovascular Physiology Concepts.* Retrieved January 12, 2011 from `http://www.cvphysiology.com/Arrhythmias/A006.htm`.

[10] Klabunde, Richard E. (2007). "Action Potentials." *Cardiovascular Physiology Concepts.* Retrieved January 12, 2011 from `http://www.cvphysiology.com/Arrhythmias/A010.htm`.

[11] "Laboratory IX: Human Cardiovascular Activity." Retrieved January 12, 2011 from http://www.bioen.utah.edu/faculty/sri/lab8_humancardiovascular.htm.

[12] Oxford Cardiac Pharmacology (2006). "Repolarisation Assays: Ventricular Myocytes: Stability of Action Potential Duration under Control Conditions." Retrieved September 23, 2010 from http://www.ocp.ltd.uk/ap10.html.

[13] Hird, R. Barry and et al (1994). "The Direct Effects of Protamine Sulfate on Myocyte Contractile Processes." *Journal of Thoracic Cardiovascular Surgery.* Vol. 108. 1994. 1100-1114.

[14] Wang, P.K.C, and B.Y. Kogan (2007). "Parametric study of the Nobles action potential model for cardiac Purkinje fibers." *Chaos, Solitons, and Fractals.* Vol. 33. 2007. 1048-1063.

[15] Winslow, Raimond L., Sonia Cortassa, and Joseph L. Greenstein (2005). "Using Models of the Myocyte for Functional Interpretation of Cardiac Proteomic Data." *Journal of Physiology.* Vol. 563.1. 2005. 73-81.

[16] Kuegler, Philipp. "Some Remarks on Singular Perturbation Theory." *Industrial Mathematics Institute.* Retrieved December 09, 2010 from http://www.tbi.univie.ac.at/~svrci/Leere/PDF/singpert-pp4.pdf.

[17] Tzitzouris, James A. "Notes on Perturbation Techniques for ODEs." *American Mathematical Society.* Retrieved December 09, 2010 from http://www.ams.jhu.edu/~castello/Applied-Math/perturbation-notes.pdf.

[18] Mehraban, Arash (2011). "Non-Classical Symmetry Solutions to the Fitzhugh Nagumo Equation." [Johnson City, Tenn. : East Tennessee State University], 2010. Retrieved September 23, 2010 from http://libraries.etsu.edu/record=b2314551~S1a.

[19] Wen, H., Brehm, P.(2010). "Paired Patch Clamp Recordings from Motor-neuron and Target Skeletal Muscle in Zebrafish." *Journal of Visualized Experiments* Retrieved March 17, 2011 from http://www.jove.com/details.php?id=2351.

[20] "Denis Noble." (2005) *Oxford Cardiac Electrophysiology Group* Retrieved April 26, 2011 from http://noble.physiol.ox.ac.uk/People/DNoble.

[21] Fenton, Flavio H. and Elizabeth M. Cherry (2008) "Models of Cardiac Cell." *Scholarpedia* Retrieved September 25, 2011 from http://www.scholarpedia.org/article/Models_of_cardiac_cell#Guinea_pig_models.